



Computer simulation of adaptive optical systems

Bolbasova L.A., Lukin V. P., Konyaev P.A.

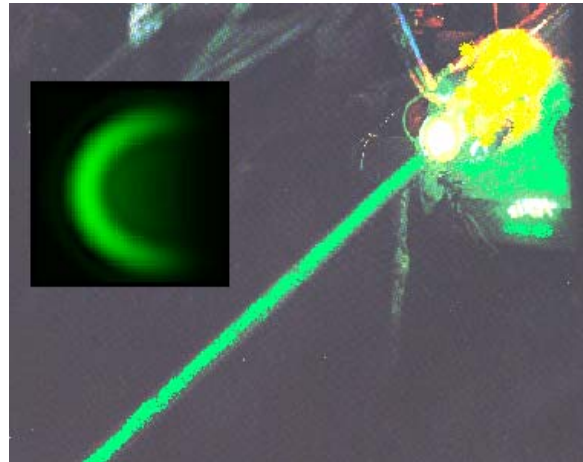
*V.E. Zuev Institute of Atmospheric Optics SB RAS
Tomsk, Russia*

Short history of development of adaptive optics theory

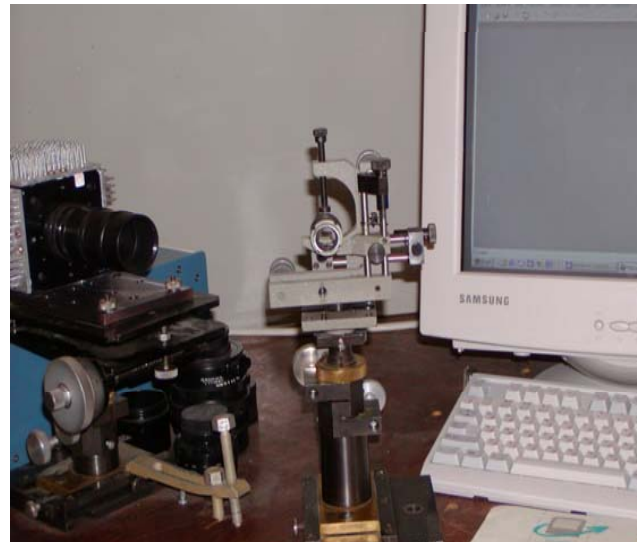
- In 1986 I completed work at monograph (English translation)
- *Lukin V.P. Atmospheric Adaptive Optics. SPIE Press. 1996.*
- which developed the theory of adaptive correction of laser beams and images in the atmosphere as a turbulent, absorbing, and refractive medium.
- **A) aspects of two-color adaptive system**
- *Lukin V.P. Efficiency of some correction systems // Optics Letters. 1979. V.4. No.1. pp.15-17.*
- **B) applying an artificial reference source (1979-1983) for image correction**
- *Lukin V.P. Correction of random angular displacements for optical beams // Quantum Electronics. 1980. V.7. №6. pp.1270-1279.*
- *Lukin V.P., Matuchin V.F. An adaptive image correction // Kvantovaja Electronika. 1983. V.10. No.12. pp.2465-2473.*
- **C) dynamic characteristics of adaptive optical systems (1986)**, where the ideas of “predicting” fluctuations for adaptive system operation were used for the first time
- *Lukin V.P., Zuev V.E. Dynamic characteristics of optical systems // Applied Optics. 1987. V.27. No.1. pp.139-147.*

The main elements of adaptive optics system simulation

Atmospheric path for propagation



adaptive mirror



wavefront sensor



1. Basic equations

- Our 4-dimensional computer code based on the a set of parabolic equations for wave propagation

$$\left\{ \begin{array}{l} 2ik \frac{\partial E}{\partial z} = \left(\frac{\partial^2}{\partial x^2} + \frac{\partial^2}{\partial y^2} \right) E + 2k^2 (n-1) E - 2ik \sqrt{\alpha_{ext}} E, \\ -2ik \frac{\partial E_r}{\partial z} = \left(\frac{\partial^2}{\partial x^2} + \frac{\partial^2}{\partial y^2} \right) E_r + 2k^2 (n-1) E_r - 2ik \sqrt{\alpha_{ext}} E_r, \end{array} \right.$$

with the boundary conditions for corrected beam and reference beam

$$E(x, y, z = o, t + \tau_d) = \sqrt{I(x, y)} \cdot \exp\left(ik \frac{x^2 + y^2}{2f} + i\varphi_c\right),$$

$$E_r(x, y, z = f, t) = R(x, y, t) \cdot E(x, y, z = f, t),$$

where $\varphi_{\tilde{n}} = A\{E_r(x, y, z = o, t)\}$ corrected phase, τ_d is lag (delay) of control induced by adaptive system, A is adaptive system operator, R is coefficient of target reflection or Rayleigh backscattering, α_{ext} is a coefficient of extinction of radiation.

2. NUMERICAL MODEL OF ADAPTIVE SYSTEM

1. WAVE-FRONT SENSOR

a) ideal phase sensor (in E_r lower index r is dropped)

$$\varphi_c = \arg(E)$$

b) ideal phase-difference sensor (below - simply ideal sensor).

$$4\varphi_{i,j} - \varphi_{i+1,j} - \varphi_{i-1,j} - \varphi_{i,j+1} - \varphi_{i,j-1} = \Delta_{i-1,j}^x + \Delta_{i,j-1}^y - \Delta_{i,j}^x - \Delta_{i,j}^y,$$

$$i, j = 1, \dots, N$$

N is dimension of calculational grid.

$$\Delta_{i,j}^x = \arg(E_{i+1,j}E_{i,j}^*), \Delta_{i,j}^y = \arg(E_{i,j-1}E_{i,j}^*).$$

c) Hartmann-Shack sensor

$$\vec{g}_k = \frac{1}{P_k} \iint_{A_k} I(\vec{\rho}) \vec{\nabla} \varphi d^2 \rho = \frac{1}{P_k} \iint_{A_k} \operatorname{Re} E \cdot \vec{\nabla}(\operatorname{Im} E) - \operatorname{Im} E \cdot \vec{\nabla}(\operatorname{Re} E) d^2 \rho,$$

P_k is power incident on the subaperture A_k . g is measured phase gradient.

2. WAVE FRONT CORRECTOR

a) modal (Zernike) corrector.

$$\varphi_c = \sum_{l=1}^{N_z} a_l Z_l \left(2 \frac{x}{D}, 2 \frac{y}{D} \right)$$

D - aperture diameter.

b) flexible mirror.

$$\varphi_c = \sum_{k=1}^{73} \phi_k f \left(\frac{\vec{\rho} - \vec{\rho}_k}{d} \right), f(\vec{\rho}) = \exp(-\rho^2/w^2),$$

d is inter-actuator spacing, $w=0,575$, ρ_k is subaperture center position.

ϕ_k is phase estimation in the center of k th subaperture.

3. RECONSTRUCTION ALGORITHM FOR HARTMANN SENSOR

$$\delta = \sum_{k=1}^{73} \sum_{l=1}^6 (\phi_k - \phi_m - \Delta_{km})^2 \rightarrow \min, \quad \frac{\partial \delta}{\partial \phi_m} = 0.$$

$$\Delta_{km} = \frac{1}{2} (\vec{g}_k + \vec{g}_m)(\vec{\rho}_k - \vec{\rho}_m)$$

Structure of 4-dimensional numerical dynamic model of AOS

In the period of 1991-1995 have been developed **four dimensional numerical dynamic model** of atmospheric adaptive systems.

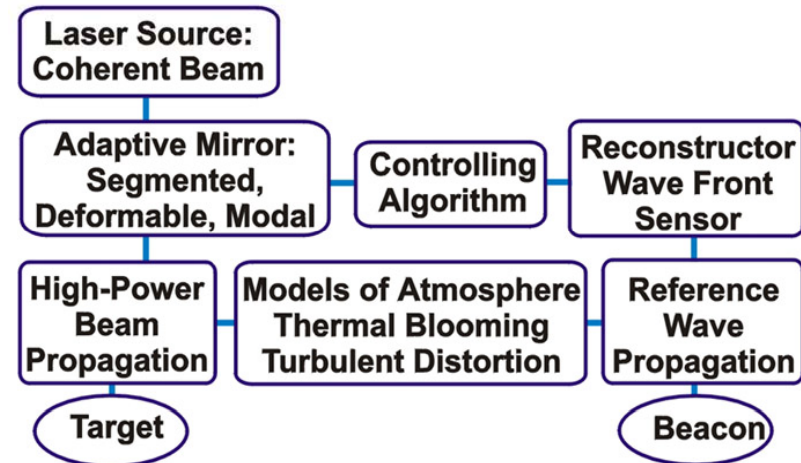
Lukin V., Fortes B. Modeling of the image observed through a turbulent atmosphere //Proc. SPIE. 1992. V.1688. pp.477-488.

Fortes B.V., Kanev F.Yu., Konyaev P.A., Lukin V.P. Potential capabilities of adaptive optical systems in the atmosphere // Journ.Opt.Soc.Am.A. 1994. V.11. No.2. p.903-907.

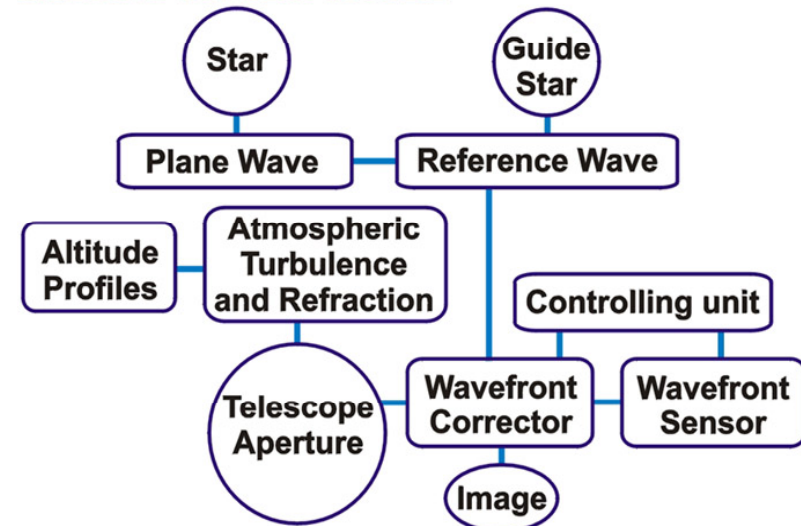
Lukin V., Fortes B. *Adaptive beaming and imaging in the turbulent atmosphere.* SPIE Press. PM109. 2002. 201 p.

STRUCTURE OF THE MODELS

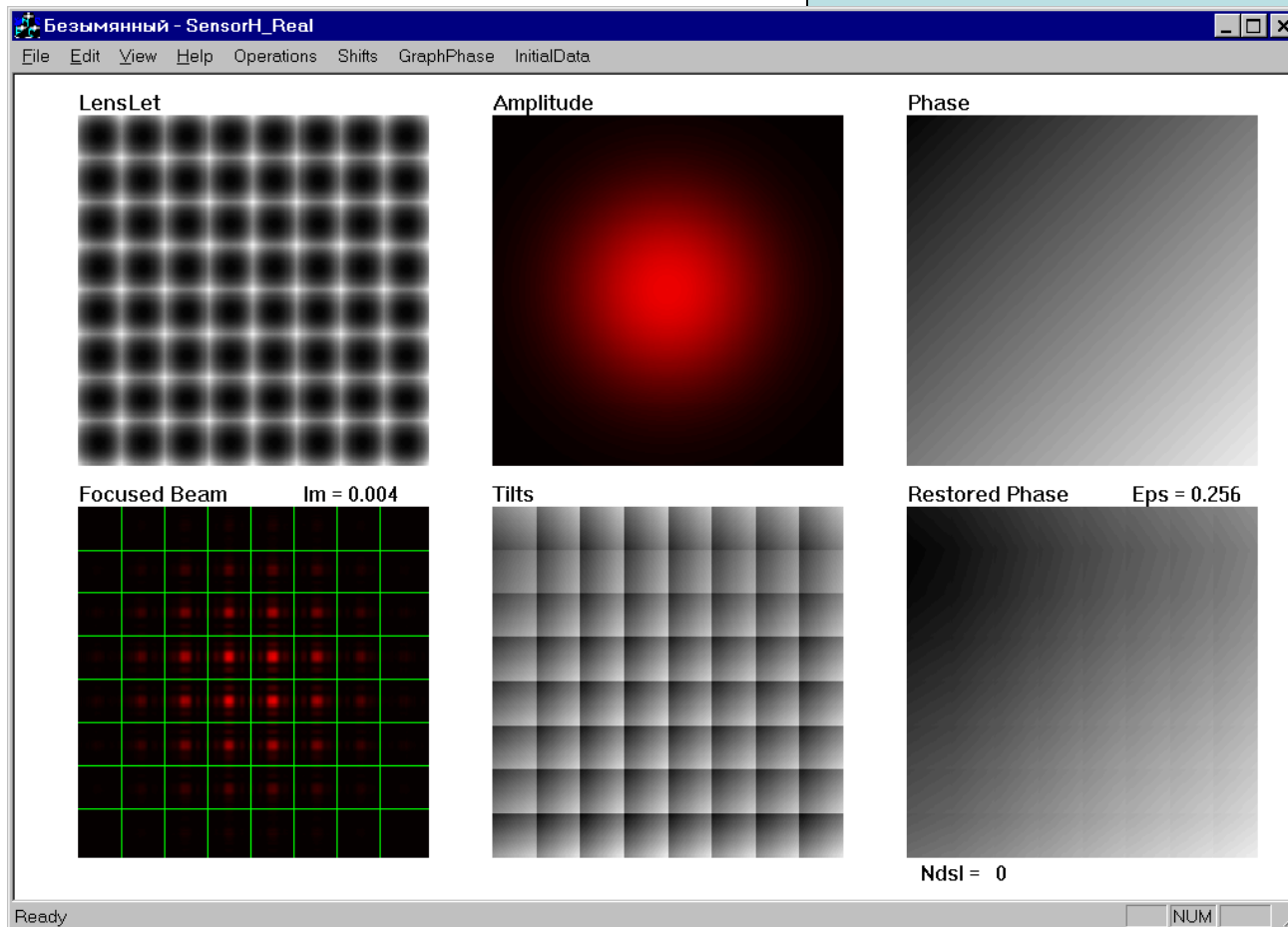
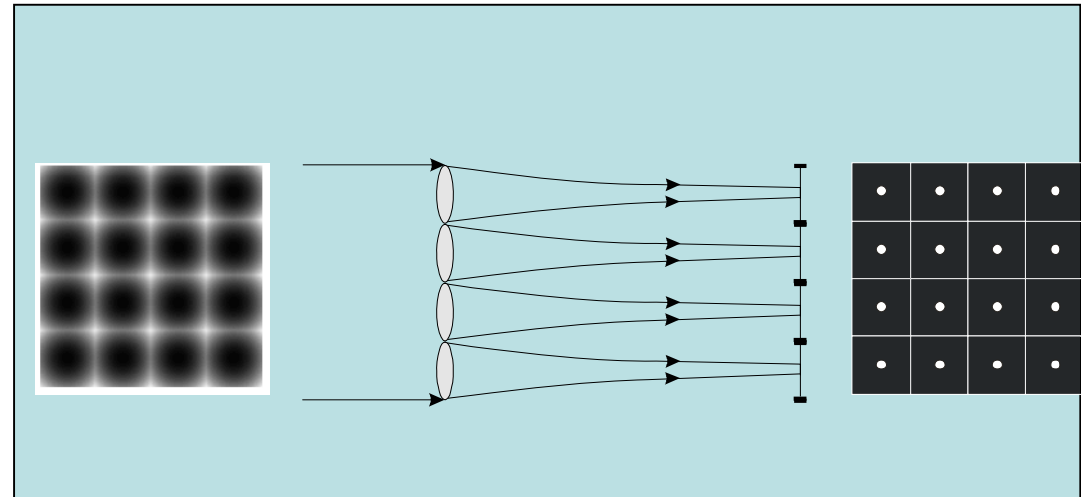
BEAMING SYSTEM MODEL



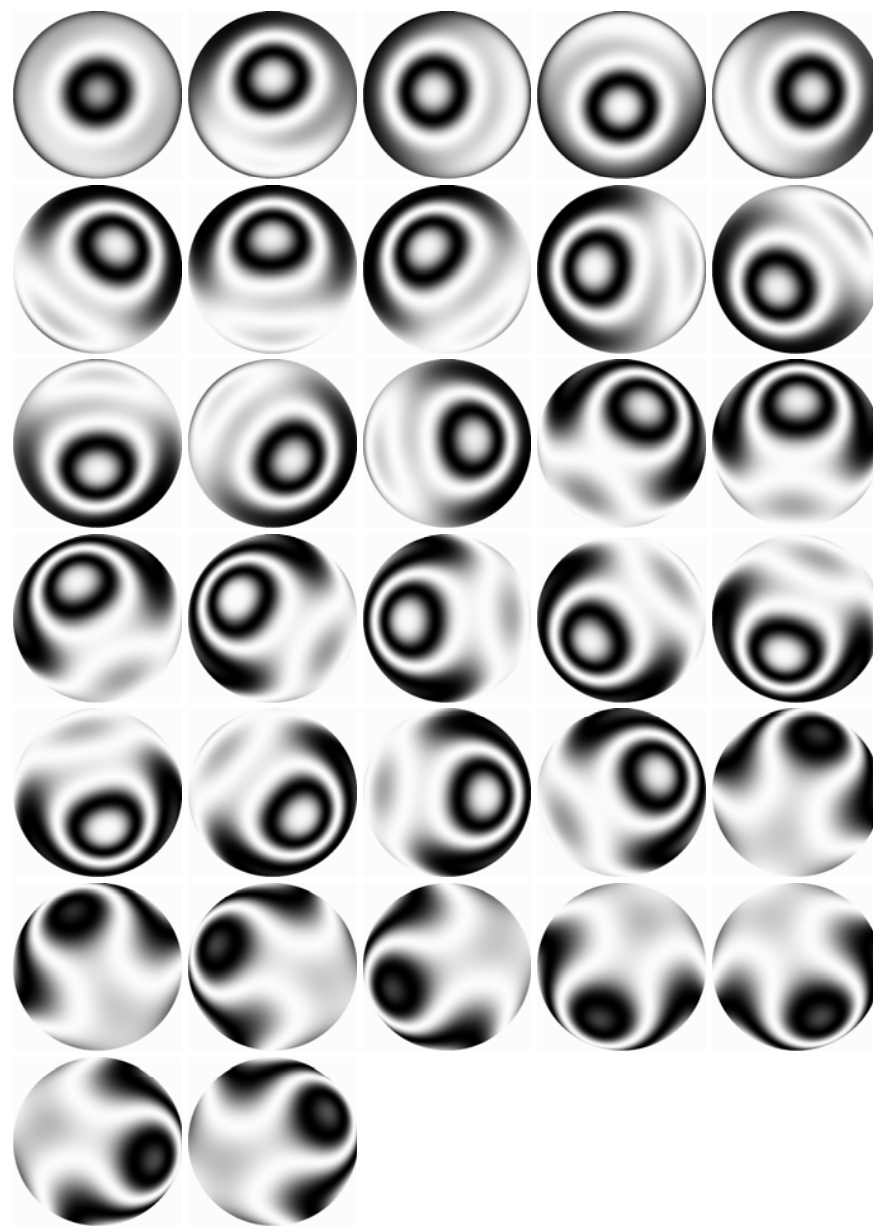
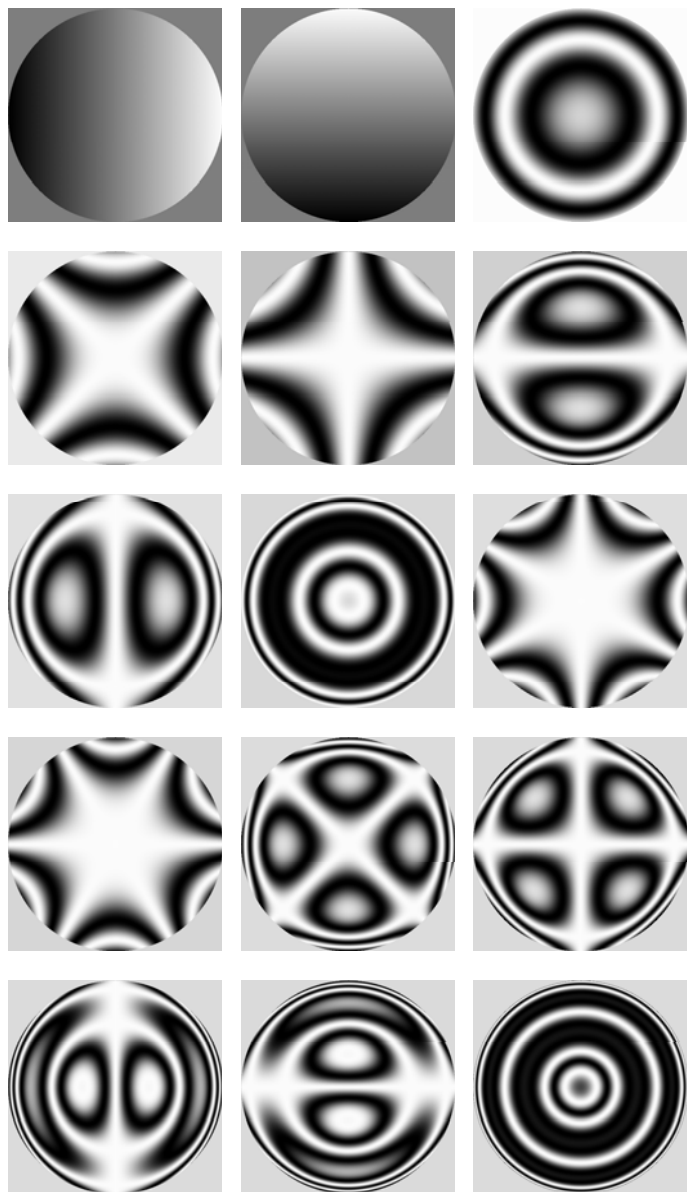
IMAGING SYSTEM MODEL



Hartmann-Shack sensor simulation



Deformable mirror: Zernike basis and a set of response functions of DM



CHARACTERISTICS OF GROUND-BASED OPTICAL TELESCOPE DUE TO ATMOSPHERIC TURBULENCE

In 1994 we completed a design project of an adaptive system for the 10-meter combined Russian telescope **AST-10**.

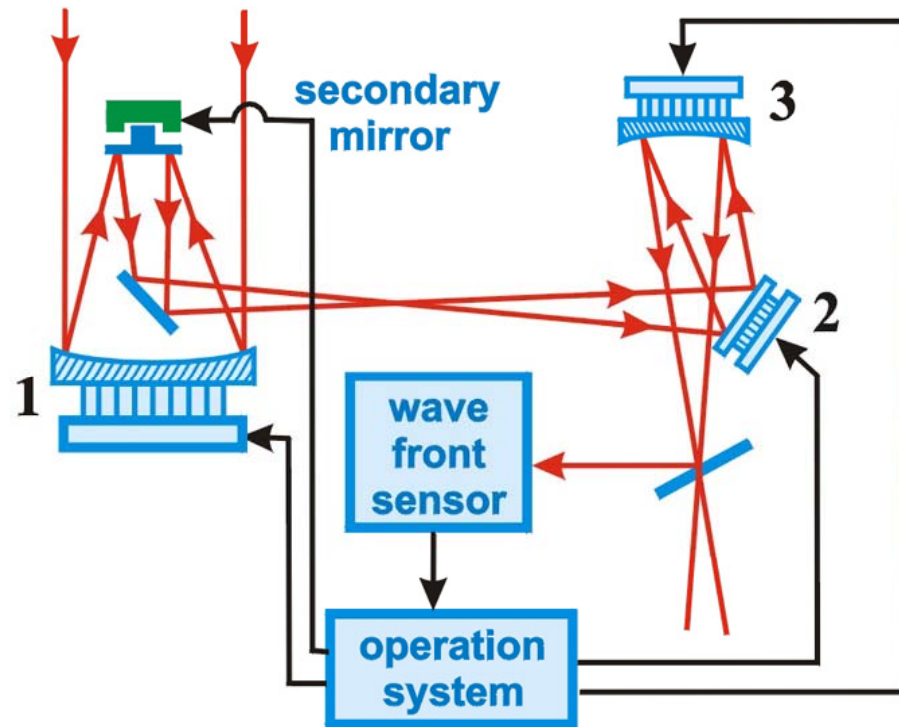
Lukin V.P. Computer modeling of adaptive optics for telescope design // ESO Workshop Proc. No.54, 1995, pp.373-378.

Lukin V.P., Fortes B.V. Partial phase correction of turbulent distortions in telescope AST-10 // Applied Optics. 1998. V.37. №21. pp.4561-4568.

Characteristics of long-base stellar interferometers were calculated (1997) with allowance for the interferometer base orientation, wind velocity distribution, and the outer scale of turbulence.

Lukin V.P., Fortes B.V. Ground-based spatial interferometers and atmospheric turbulence // Pure and Applied Optics. 1996. V.5. No.1. pp.1-11.

The structure of adaptive telescope with active primary mirror (1) and two adaptive mirrors (2, 3)



CHARACTERISTICS OF GROUND-BASED OPTICAL TELESCOPE DUE TO ATMOSPHERIC TURBULENCE

In 1994 we completed a design project of an adaptive system for the 10-meter combined Russian telescope **AST-10**.

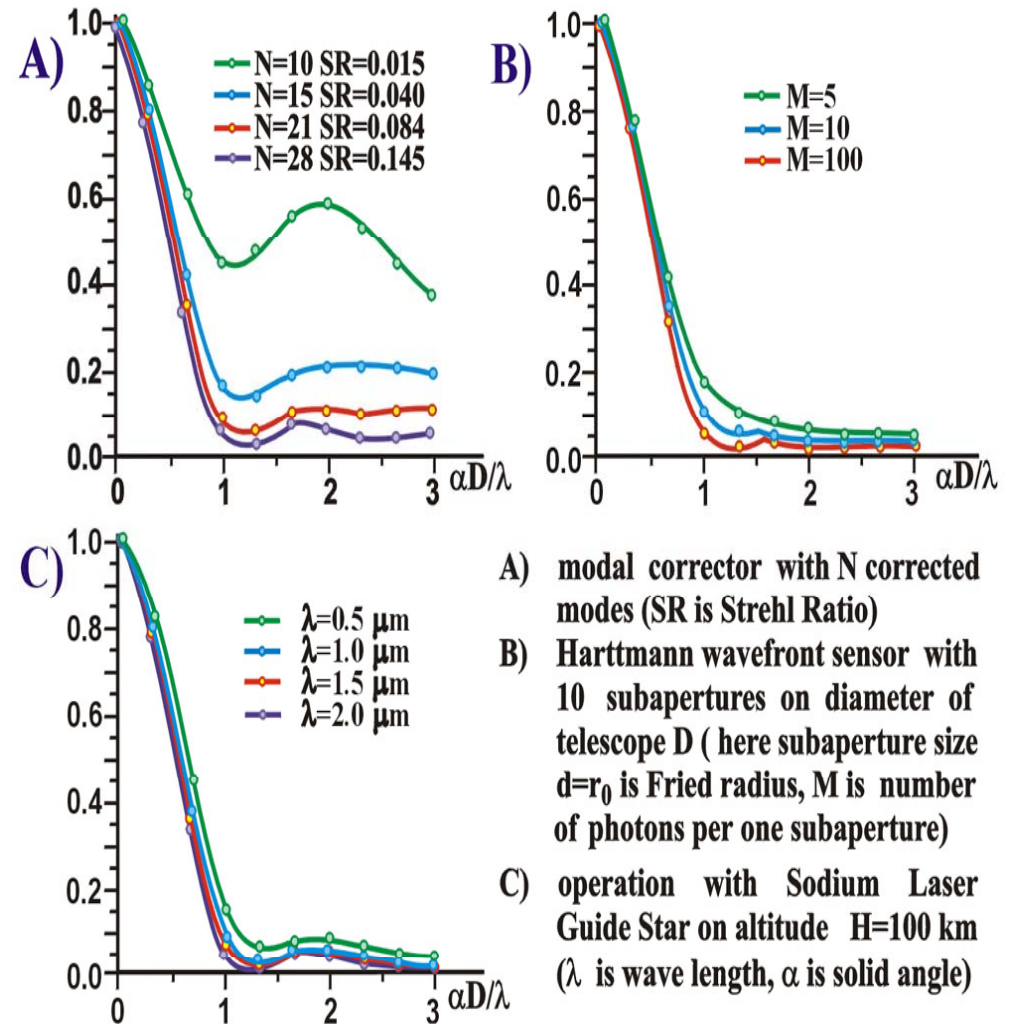
Lukin V.P. Computer modeling of adaptive optics for telescope design // ESO Workshop Proc. No.54, 1995, pp.373-378.

Lukin V.P., Fortes B.V. Partial phase correction of turbulent distortions in telescope AST-10 // Applied Optics. 1998. V.37. №21. pp.4561-4568.

Characteristics of long-base stellar interferometers were calculated (1997) with allowance for the interferometer base orientation, wind velocity distribution, and the outer scale of turbulence.

Lukin V.P., Fortes B.V. Ground-based spatial interferometers and atmospheric turbulence // Pure and Applied Optics. 1996. V.5. No.1. pp.1-11.

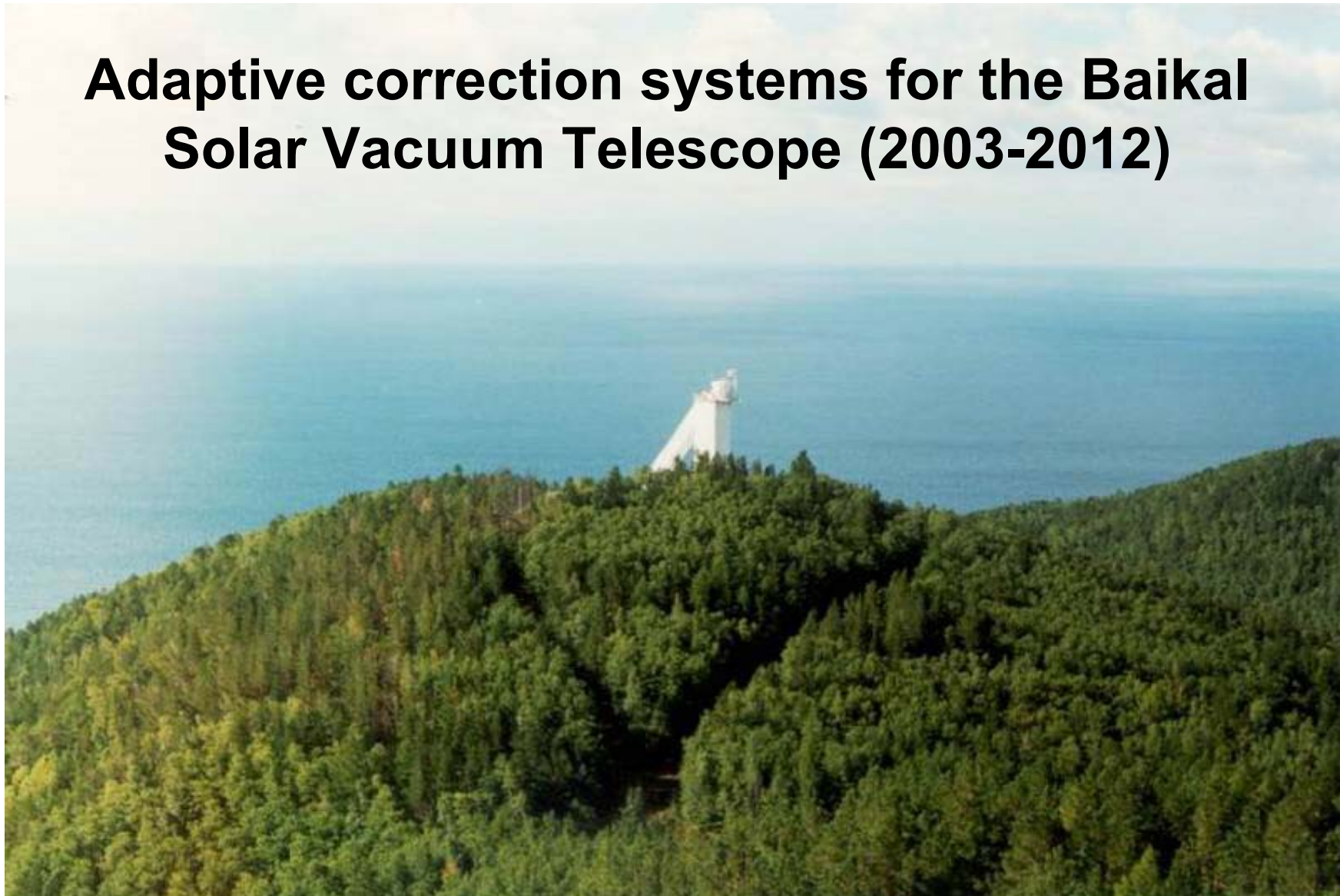
Partial Image Correction (Point-Spread Function)



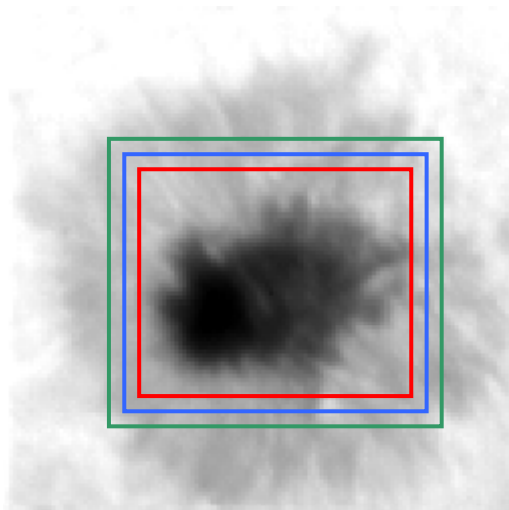
CHARACTERISTICS OF GROUND-BASED OPTICAL TELESCOPE DUE TO ATMOSPHERIC TURBULENCE

- Using an analytical algorithm for atmospheric correction the performance of the **Euro50 telescope project** is analyzed.
- The atmospheric model employed is the **ORM (Observatorio del Roque de los Muchachos) 7 layer model with an outer scale distribution.**
- The values of effective outer scale found that at apertures of modern telescopes of several meters the influence of the finite L_0 on the energy balance between tip-tilt and higher order modes must be properly taken into account.
- **Lukin V., Goncharov A., Owner-Petersen M., Andersen T.**
- **The effective outer scale estimation for Euro-50 site**
- **// Proc. SPIE. 2002. Vol.5026. pp.112-118.**

Adaptive correction systems for the Baikal Solar Vacuum Telescope (2003-2012)

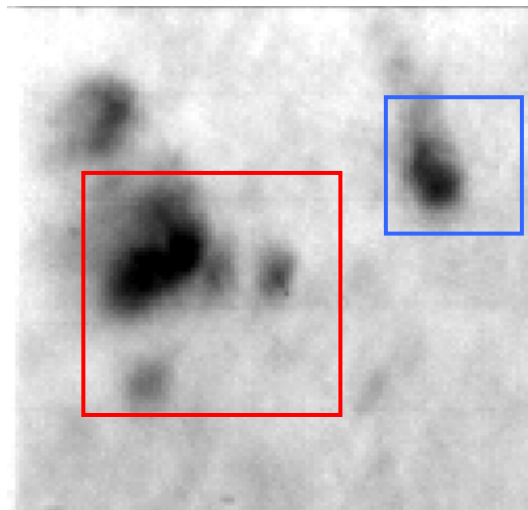


1- Sunspot



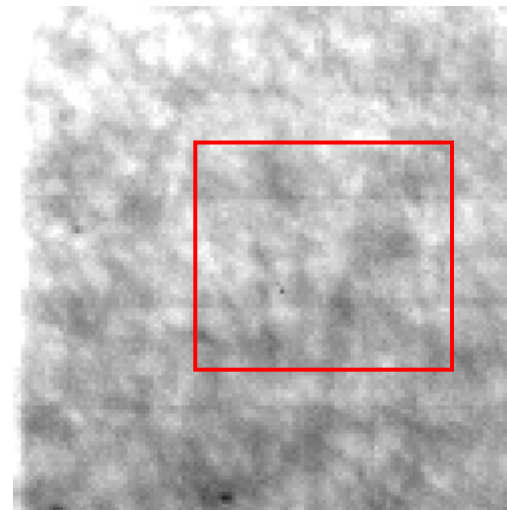
Contrast 25-30 %

2- Pores group



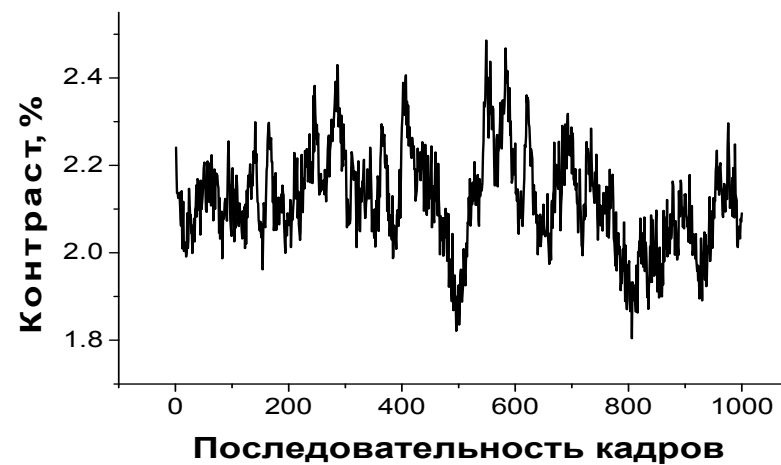
Contrast 10-15 %

3- Granulation



Contrast 1-3 %

-  Centroid tracking analog
-  Centroid tracking digital
-  Correlation tracking



Used correlation tracking algorithms

1. Correlation function

$$C(i, j) = \sum_{l=0}^{N-1} \sum_{m=0}^{M-1} I(l, m) I_R(i+l, j+m)$$

I – current frame

I_R – reference frame

2. Normalized correlation function

$$C_N = C / C_R$$

$$C_R(i, j) = \left[\sum_{l=0}^{N-1} \sum_{m=0}^{M-1} I^2(l, m) \sum_{l=0}^{N-1} \sum_{m=0}^{M-1} I_R^2(i+l, j+m) \right]^{1/2}$$

3. Correlation FFT algorithm

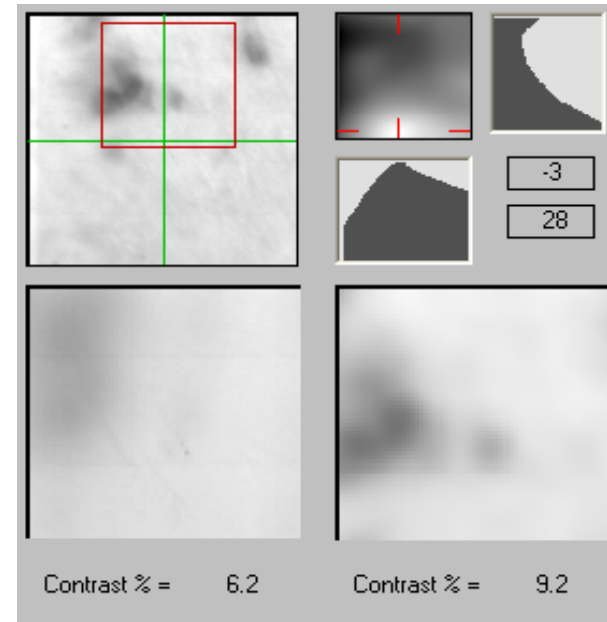
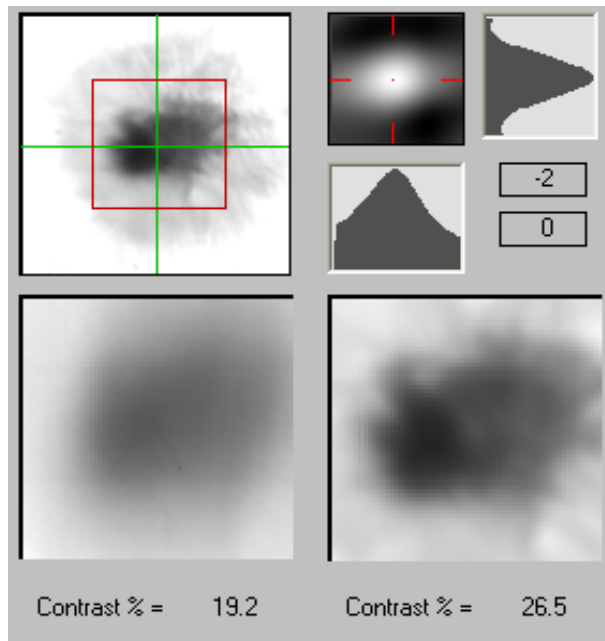
$$C = F^{-1} \{ F^+ [I] \times F^+ [I_R] \}$$

F – mixed radix FFT

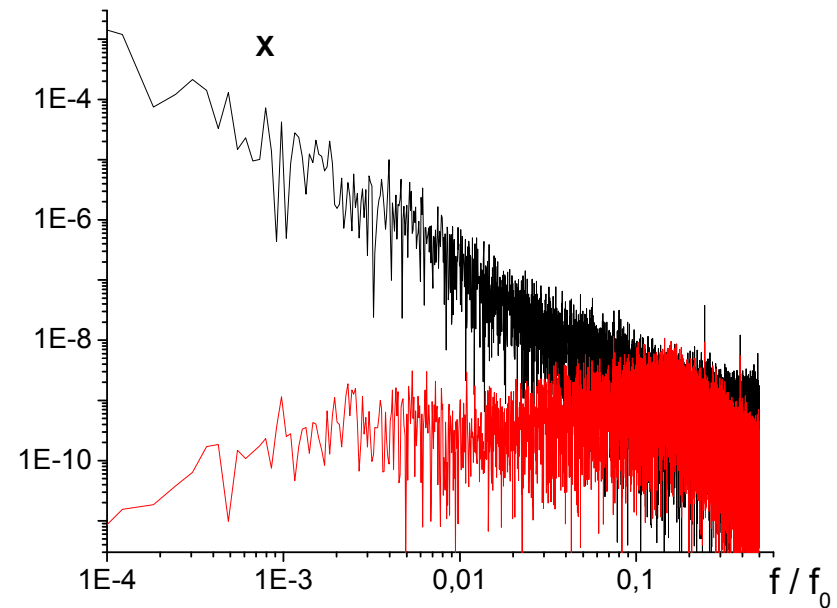
4. Modified correlation FFT algorithm (Booster)

$$C_m = F^{-1} \{ F^+ [I] \times F^+ [I_R] \times H_B(k_x, k_y) \}$$

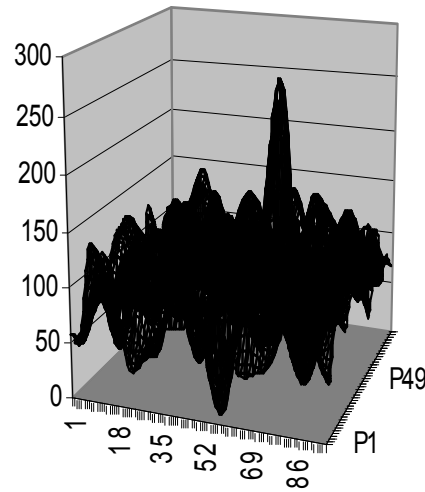
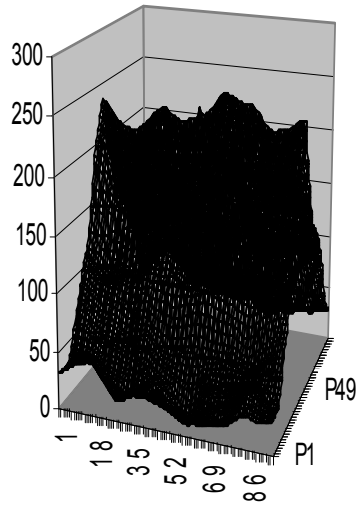
Correlation tracking of spot patterns



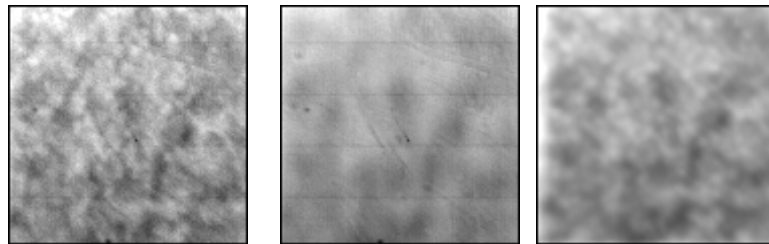
Power spectrum of non-corrected
(black) and corrected (red) image
displacement. $\sigma_2 / \sigma_1 = 24$



Modified correlation wavefront sensor (2006) is based on camera DALSA CA-D6 (260X260 pixels, pixel size 10 mkm, 12 bit, 955 fpc)

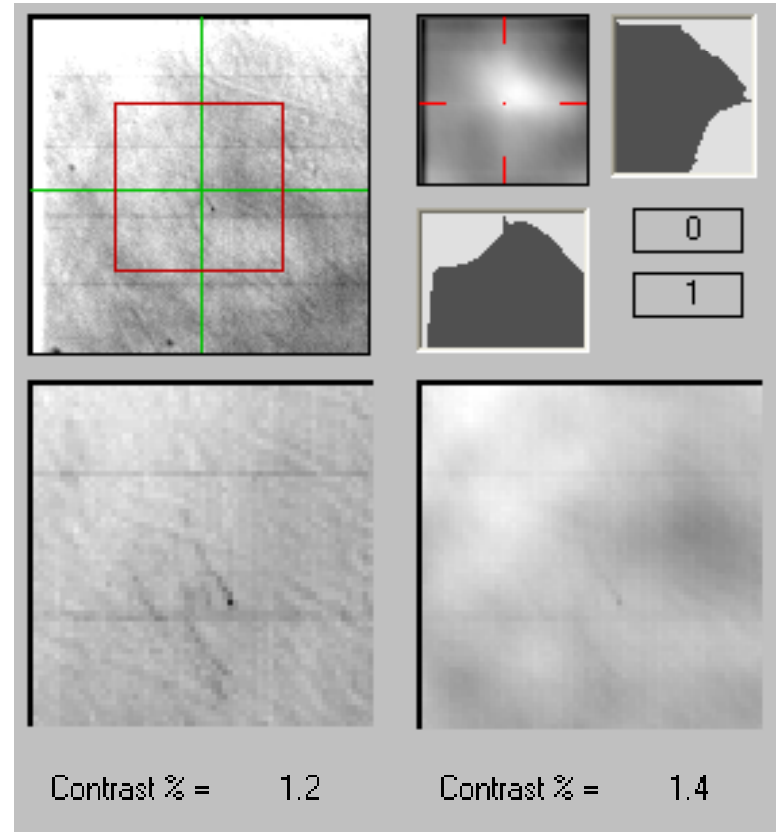
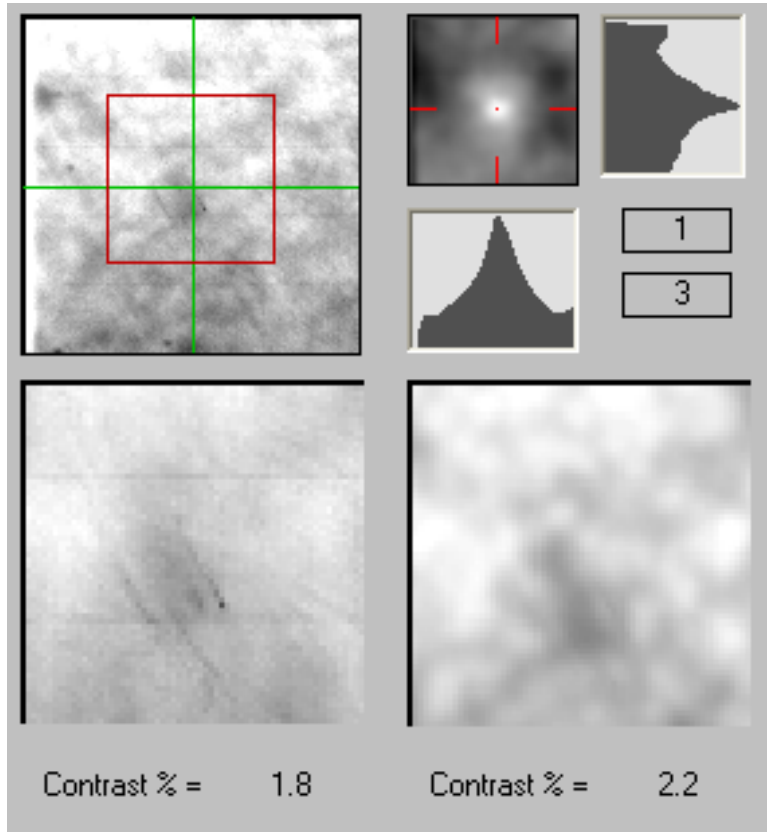


Comparison of joint correlation functions for traditional (left) and modified (right) correlation trackers.



The set of pictures for "short exposure" (2 mc), in regime of "long exposure" (2 c) without control, and in regime «long exposure» (2 c) with modified sensor.

3- Granulation



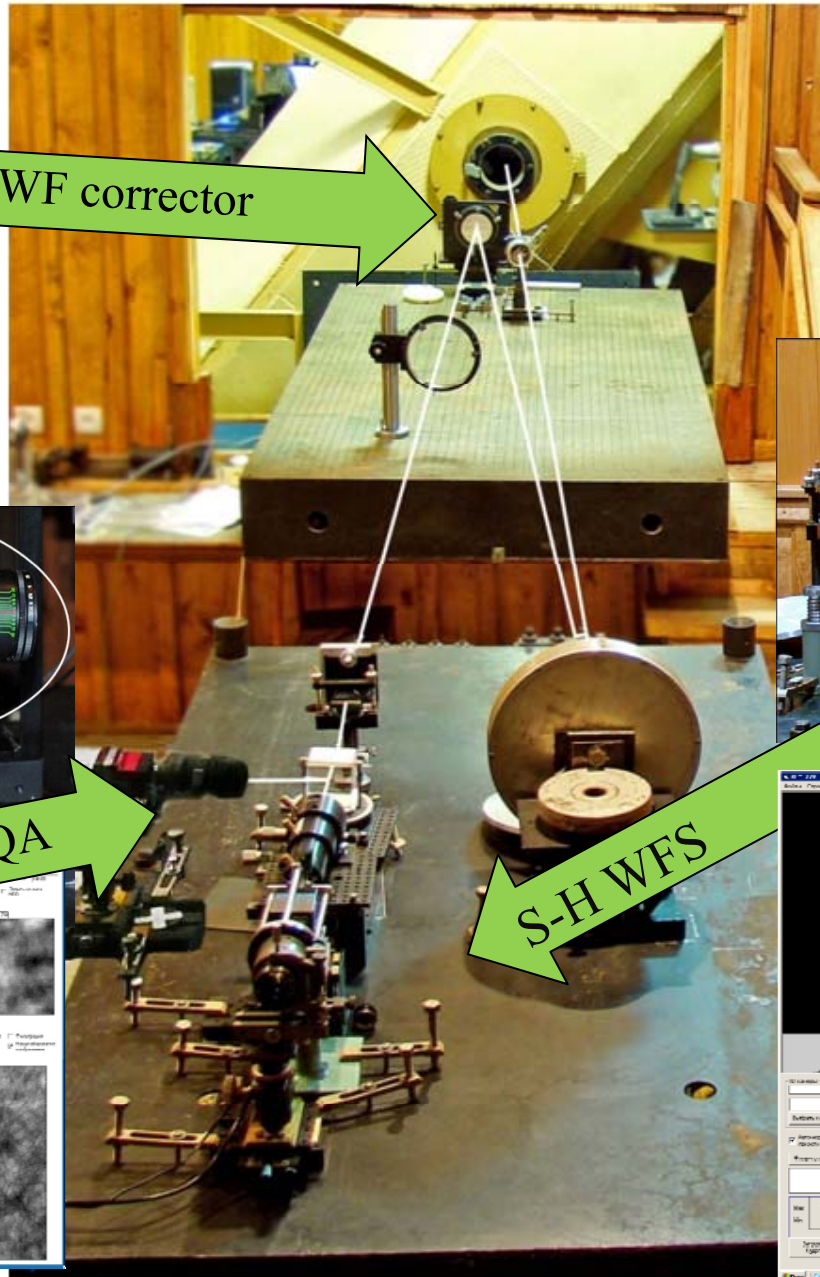
Solar tracking Systems

Country	USA	France- Italy	Spain	China	Russia BSVT
Years of operation	1989	1995	1995	2001	2001-2005
Diameter (mm)	760	900	980	430	760
Beacon	granulation	granulation	granulation	Sunspot	Sunspot/ granulation
Algorithm	cross correlation	granulation tracker	absolute difference	absolute difference	modified correlation
Sampling freq (Hz)	417	582	1350	419	164-245
Field of view	10"x10"	2"x2" ~ 12"x12"	14"x14"	5"x5" ~ 20"x20"	33"x33"
Bandwidth	25 Open loop	60 Close -3dB	100 Open loop	84 open loop 30 close -3dB	120 Open loop
Image quality	Motion 0.023" rms	Resolution 0.2"	Motion 0.05" rms	Motion 0.14" rms	Motion 0.07" rms

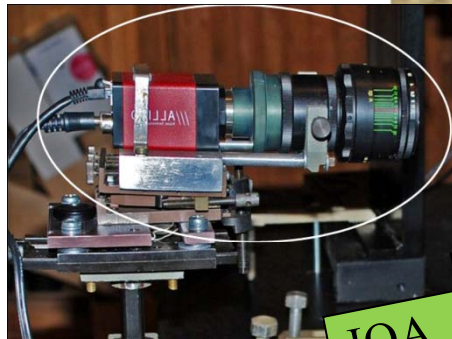
Present view of adaptive system ANGARA on the Big Solar Vacuum Telescope (Baikal Astrophysical Observatory, 2009)



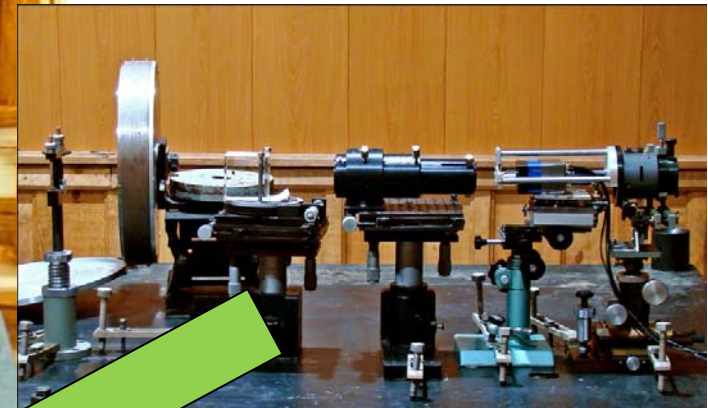
WF corrector



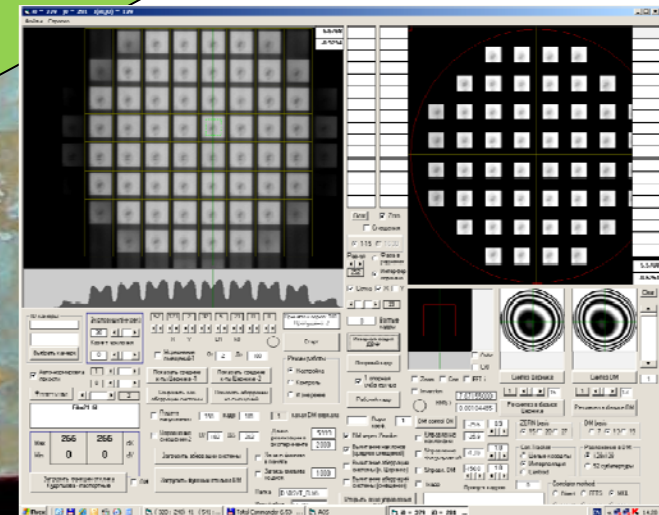
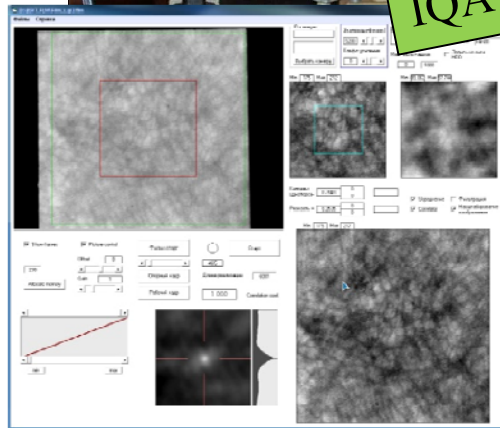
RF patent on useful model
«Telescope with adaptive optical system» № 111695
(priority at 29.06.2011,
IAO SB RAS, ISTP SB RAS)



IQA

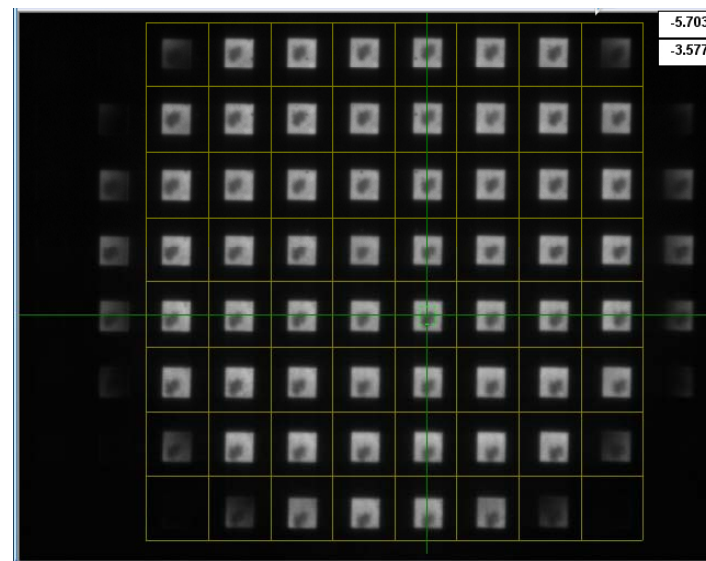
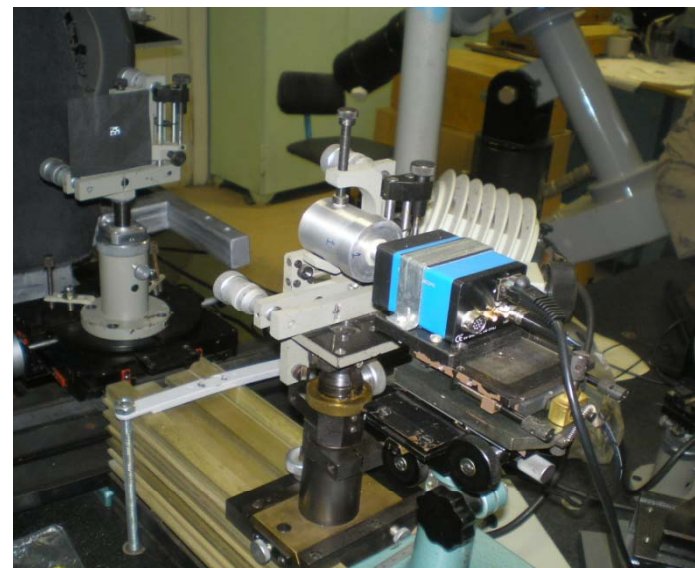


S-H WFS



Correlation S-H wavefront sensor

- This sensor use the extended object images as a source of measurement, as well as solar spots, pores, and solar granularities.
- Sensor consist from the raster of square diffractive lenses with numerical aperture 0.019 and video-camera GE680 Prosilica (Canada) with resolution 640x480 pixels (size of 1 pixel is 7.4 μm).
- This device is suitable to measure wavefront distortions with error below **1/60 of wavelength.**
- Wave-front sensor of FOW not more than
- 40 arc. sec.
- Botygina N.N., Emaleev O.N., Konyaev P.A., Lukin V.P. Wavefront sensors for adaptive optical systems //Measurement Science Review. 2010. V.10. №3. P.101.



Deformable mirror /adaptive system ANGARA



Bymorph mirror



Amplifier, one channel



Mirror , back view

Base of AOS simulation - technologies of parallel programming

Set-ups for parallel programming:

INTEL Math Kernel Library (MKL) v.10.3
INTEL Integrated Performance Primitives (IPP) v.7.0
NVIDIA CUDA Toolkit 4.01

Basic functions of library MKL:

Vector and matrix algebra
Statistics and random number generators
Fast Fourier Transformation (1-D, 2-D, 3-D)

Basic libraries of IPP:

Signal processing (convolution, correlation)
Images processing (filtration, digital transformations, coding and decoding)

Basic functions of library CUDA:

Vector and matrix algebra
Statistics and random number generators
Fast Fourier Transformation (1-D, 2-D, 3-D)

Two parallel algorithms, using **OpenMP technology with MKL library for Intel multicore processors**

and

CUDA technology for NVIDIA graphic accelerators

have been created.

Methods and features of **parallel algorithms** for numerical simulation of optical waves propagation are considered. The **scalar parabolic equation** for a complex amplitude of monochromatic waves was solved numerically, using the Fourier transform method for homogeneous media and **split-step Fourier method** for inhomogeneous media.

$$2ik \frac{\partial U}{\partial z} + \left[\frac{\partial^2}{\partial x^2} + \frac{\partial^2}{\partial y^2} + 2k^2 n_1(x, y, z) \right] U = 0$$

$$\frac{\partial U}{\partial z} = [L_D + L_R] U \quad L_R = ikn_1(x, y, z) - \text{refraction_operator}$$
$$L_D = \frac{i}{2k} \left[\frac{\partial^2}{\partial x^2} + \frac{\partial^2}{\partial y^2} \right] - \text{diffraction_operator}$$

Konyaev P.A., Tartakovskii E.A., Filimonov G.A. Computer simulation of optical waves propagation, using parallel programming technique // Atmospheric and Oceanic Optics. 2011. V. 24, No.05. P. 359-365 [in Russian].

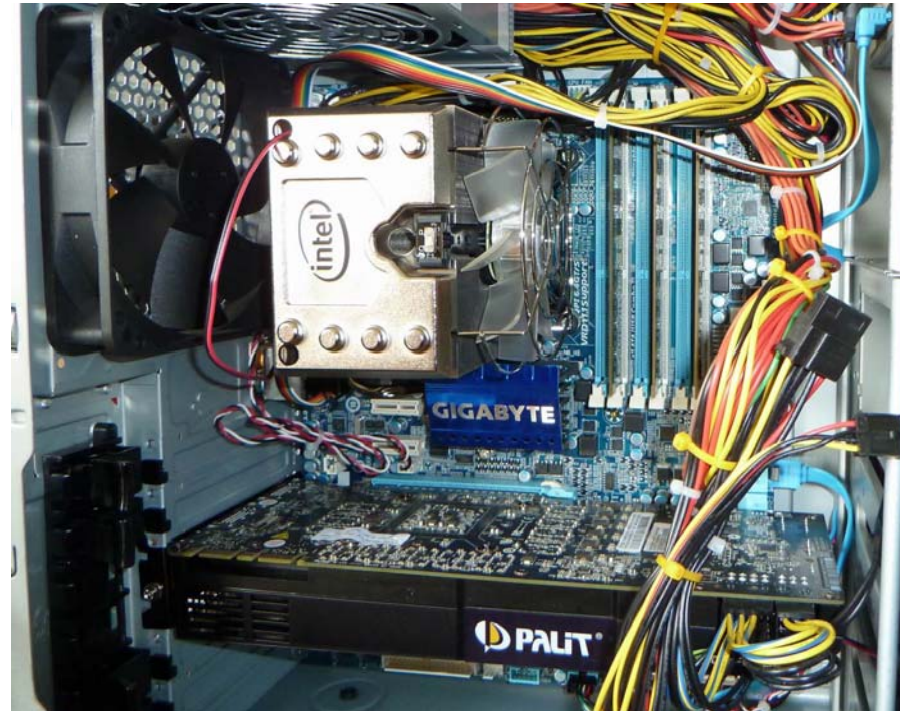
The hardware system for computer simulation is an off-the-shell

desktop with

6- core 12-thread Intel Core i7-980 at the maximum frequency of 3.6 Ghz Turbo boost and an NVIDIA GeForce GTX 590 graphic accelerator with 1024 universal processors operating at 1.5 Ghz.

- Model SIMD (one team – many data, graphic memory 3000 Mb)
- Interface OpenMP (Intel) and CUDA (Compute Unified Device Architecture).

OS Linux, Windows, MS Visual Studio, NVIDIA CUDA Toolkit 4.x, plugin for MATLAB



The comparison of two parallel approaches with each other and with a common sequential algorithm

Using FFTW library, was performed by calculation of average number of test task solutions per second. It is shown that parallel algorithms have a considerable **advantage in speed (by tens times)** to the common sequential algorithm in accordance with the grid size in computational task. When comparing the performance of the above two parallel techniques with each other the results were as follows: for grids up to 1024X1024 the approach, using **OpenMP technology**, holds the lead, while for the large grids (from 1024X1024 and more) the approach, using **CUDA technology** was faster.

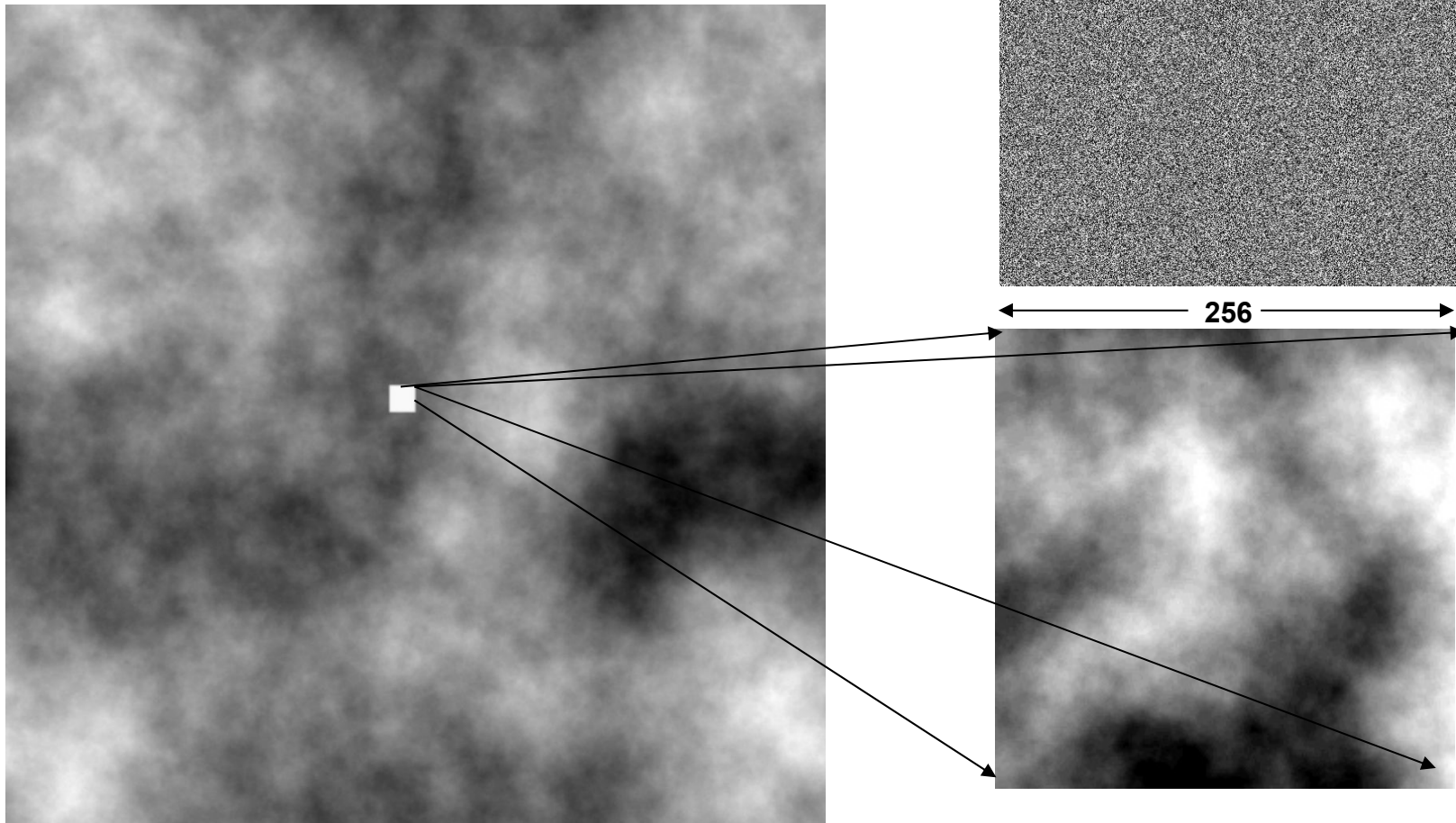


Turbulence with large scales of sizes

- Spectral method (2-D FFT MKL, CUDA, IPP):
- - model of turbulence with large scales of sizes $\sim 1:10000$
- - modern generators of uncorrelated numbers with large period (linear congruent sensor from standard library $\sim 2^{31}-1$) 
- - simulation of large scale optics with high resolution
- - dynamic model of turbulence for AOS modeling

SIMD-oriented fast Mersenne Twister random generator *SFMT19937* (Intel MKL) with period $=2^{19937}$

8192



Correlation S-H wavefront sensor portal for solar telescope

$i_0 = 372$ $j_0 = 264$ $I(i_0, j_0) = 80$

Файлы Справка

-5.7031	0.0000	0.00000
-3.5775	0.0000	0.00000
	1.5044	1.54677
	-2.7044	-2.70982
	2.1833	2.15452
	-0.5537	-0.55975
	0.8579	0.76724
	0.5607	0.58161
	0.5231	0.48701
	0.1298	0.12351
	0.0224	0.41231
	-1.5466	-1.54191
	0.1416	-0.04041
	-1.5338	-1.43416
	-0.0168	-0.01072

0.64569
-0.16031
-0.49621
-0.35137
-0.29753
0.30084
-0.77336
-0.70527
-3.71500
-4.80533
-0.91800
-2.45758
-3.37843
-0.34075
-1.79246
-3.00908
-0.11933
-3.36169
-2.45699

Clear Zern
 Смещения

1-15 16-30
Радиус 274 Фаза в радианах
Интерферограмма

Сетка X Y

31

1 Взяты кадры

Инициализация ДВФ

Опорный кадр

1 опорная субапертура

Рабочий кадр

Порог коэф.

DM через Zernike

Вычитание наклонов (средних смещений)

Вычитание aberrаций системы (к. Цернике)

Вычитание aberrаций системы (смещений)

Открыть окно управления DM

Zoom Corr FFT-i

Inversion PMS->

DM control ON -18 0.5

Управление наклонами -18

Управление фокусировкой -7.66

Упр. DM -150.0 1.0

Пропуск кадров 0

ZERN basis 15 20 27

DM basis 7 13 19

Corr. Tracker
 Целые координаты
 Интерполяция
 Centroid

Разложение в DM:
 128x128
 52 субапертуры

Correlator method:
 Direct FFTS MKL
 CUDA Batch IPP

ID камеры: Экспозиция(мксек) 57 116 8 16 5 31 0 0
Кадров: всего 2876 принято 102
Кэф-т усиления 5219
Выбор камеры: 0
Авто-нормировка яркости: 1
Фильм старт: 334
пятно 5000d 7 vac 2.fil
Max 255 255 dx
Min 0 0 dy
Загрузить функции отклика Кудряшова - паспортные
Загрузить функции отклика DM
Папка D:\BSVT_FLM\
Имя файла Film00

Усреднение смещений-1 От 2 До 100
Усреднение смещений-2 От 102 До 202
Длина реализации в эксперименте 3000
Запись фильма в память 1000
Запись фильма на диск
Поддача напряжения 150 кадр 101 1 канал DM-зеркала
Режим работы: Настройка Контроль Измерение

Показать средние к-ты Цернике -1 Показать средние к-ты Цернике -2
Сохранить как aberrации системы Показать aberrации из смещений

Подача напряжения Усреднение смещений-1 Усреднение смещений-2

DM через Zernike Вычитание наклонов (средних смещений) Вычитание aberrаций системы (к. Цернике) Вычитание aberrаций системы (смещений)

DM Corr FFT-i Inversion PMS->

DM control ON Управление наклонами Управление фокусировкой Упр. DM

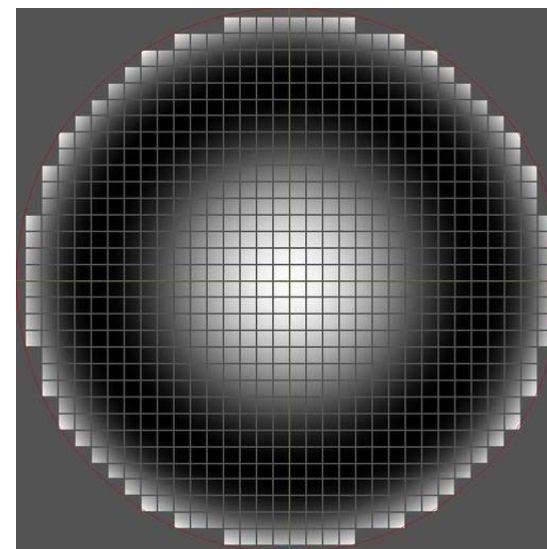
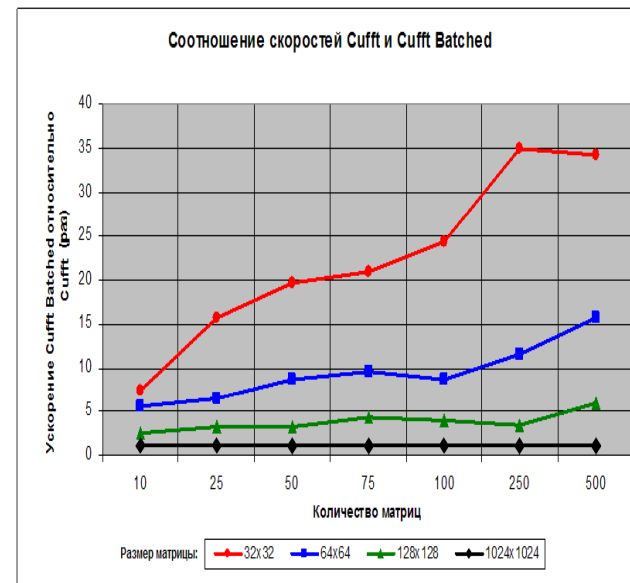
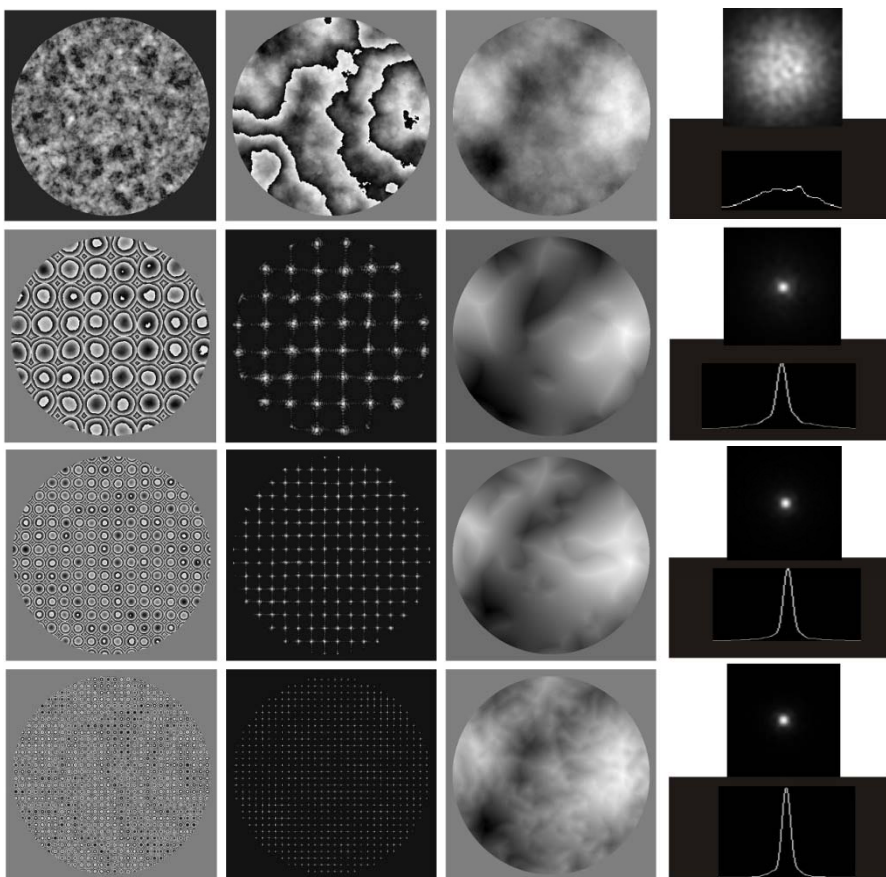
ZERN basis DM basis Corr. Tracker

Direct FFTS MKL CUDA Batch IPP

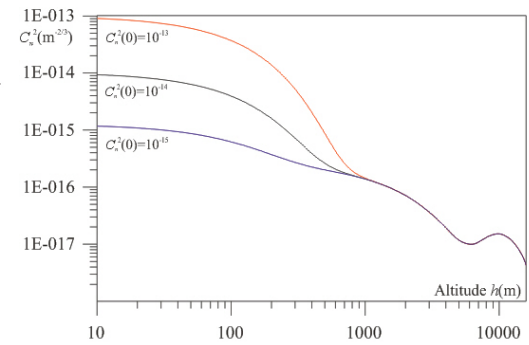
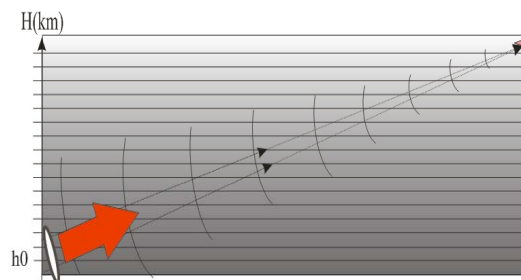
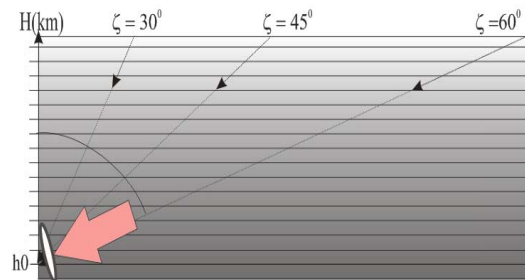
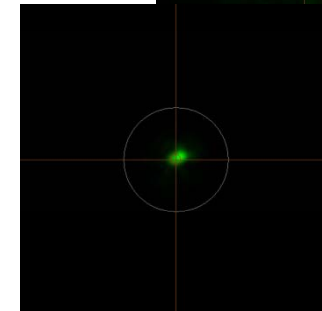
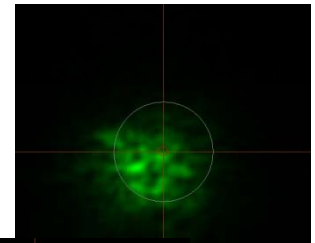
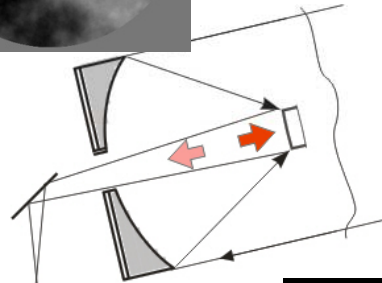
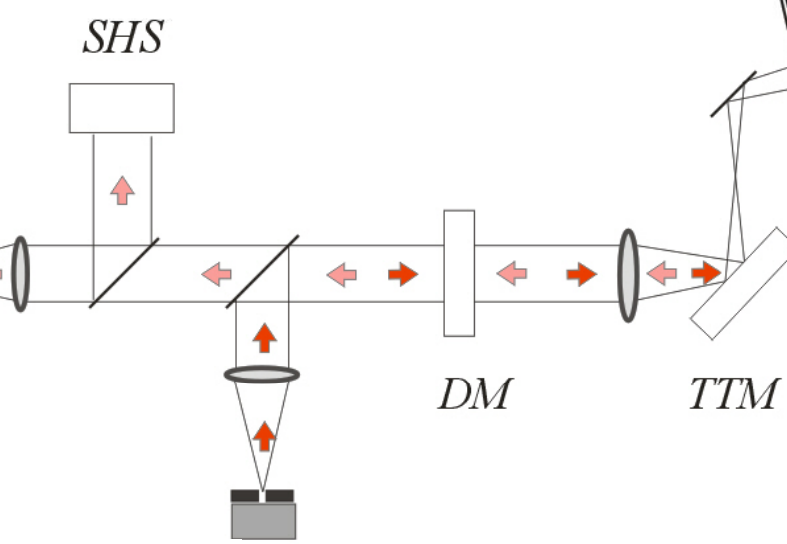
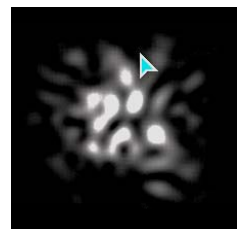
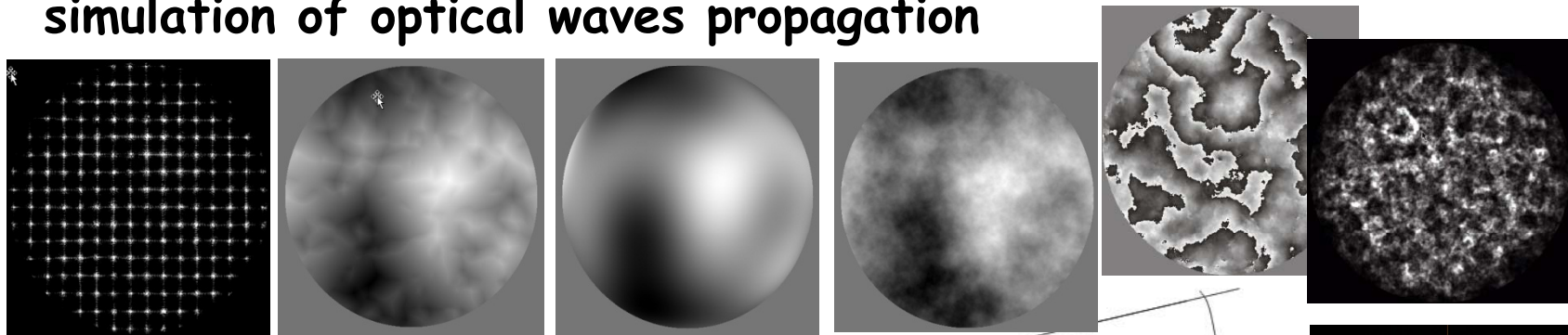
Вычитать дефокусировку Z(3)->defocus Closed loop control

Measurements of wavefront: S-H wavefront sensor

- Technology of CUDA Batched Processing (extended model of SIMD)
- Parallel algorithms of Hartmannograms processing
 - Two-dimensional correction with parallel 2-D FFT,
 - Parallel multiplication vector by reconstruction matrix
 - Parallel algorithm of Fourier demodulation
- Modeling of extremal wave-front sensors



Parallel programming technique for computer simulation of optical waves propagation



A modified spectral-phase algorithm for computer simulation of time-evolving turbulence in atmospheric and adaptive optics applications

Known spectral-phase method for computer simulation of random processes and fields with given spectral densities. For 2-D discrete field this method may present as

$$\begin{aligned} s(i, j) &= \sum_{l=0}^{L-1} \sum_{m=0}^{M-1} S(l, m) \exp(\mathbf{i}g(l, m)) \exp\left[\mathbf{i}2\pi\left(\frac{li}{L} + \frac{mj}{M}\right)\right] = \\ &= FFT\{S(l, m) \exp(\mathbf{i}g(l, m))\}. \end{aligned}$$

Here *FFT* is operator of discrete Fourier transformation, $g(l, m)$ is a 2-D random field (“white noise”); $S(l, m)$ is spectral amplitude, satisfying condition

$$|S_{l,m}|^2 = \Phi(k_{l,m}) \Delta k^2, \quad k_{l,m} = \Delta k \sqrt{l^2 + m^2},$$

where $\Phi(kl, m)$ is required spectral density.

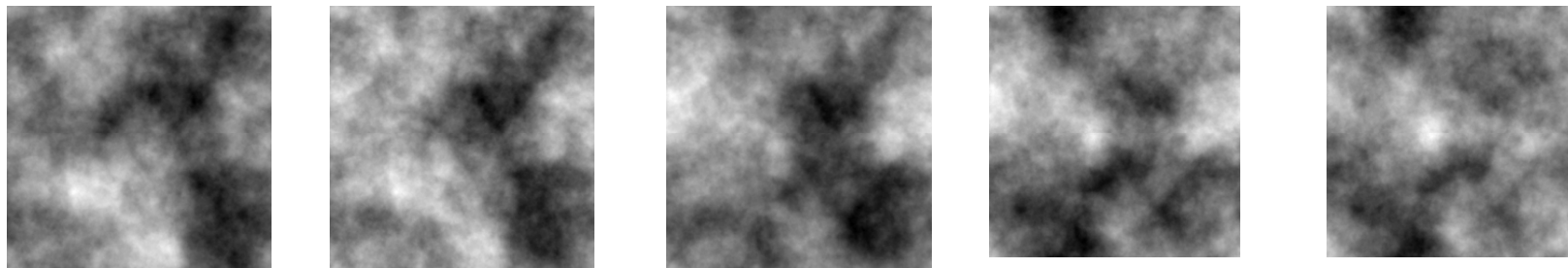
As a model of evolution of field $s(k, l)$ in time for discrete moments of time $tn = nT$, where T is interval to sampling used the model of autoregression with slitherring average, which is broadly used in theories of the random processes.

Very interesting model of 1-order, which present minimum requirements to memory of computer:

$$f(nT) = a_1 f((n-1)T) + z(nT);$$

$$z(nT) = b_1 r((n-1)T) + r(nT).$$

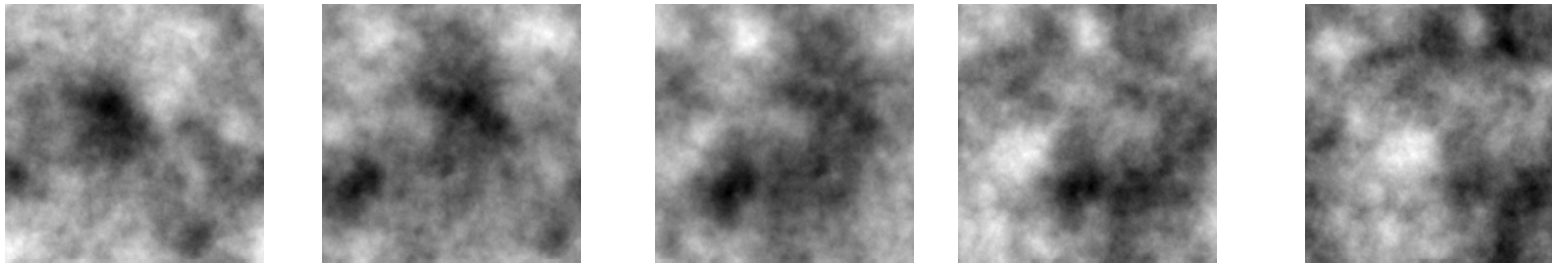
Here $r(nT)$ is descrete white noise with normal distribution, zero average and variance. **Figure below present evolution of 2-D random field $s(i, j)$ with Kolmogov's power type of model** with coefficients $a_1 = 0.999$, $b_1 = 0.9$ and variance of noise $s_2 = 0.01$. The sequence of the frames illustrates the fluent time histories, comparing first and the last frames to serieses, possible notice that occurred full change the initial frame.



- For modeling of the evolutions in media, moving at the speed of $V(V_x, V_y)$, necessary introduce exponential multiplier of the shift:

$$s(i, j) = FFT \left\{ S \exp(i g(l, m)) \exp(i n T (v_x + v_y)) \right\}.$$

- Evolution of the field is shown on Figure with same power spectrum in moving (left to right) media.



- The implementation of the algorithm is shown to be simple and efficient in simulations of dynamic problems of atmospheric and adaptive optics

Hardware-programme complex for Full Sun Telescope of Baikal Astrophysical Observatory

Complex for numerical processing and analysis of images of solar chromosphere on the base of modern technologies of parallel programming

- **List of problems**
- - analysis of images and choose the best image in different formats and transformations,
- - correction of instrumentation and atmospheric distortions, calibration, and high precision co-ordination of images,
- - spherical transformation details on Sun surface with scale changing, measure of angular of rotation, coefficient of scaling,
- - corrtensial transformation of images – поворот, масштабирование, перенос и т.д.,
- - space-temporal correlation and spectral analysis of images.

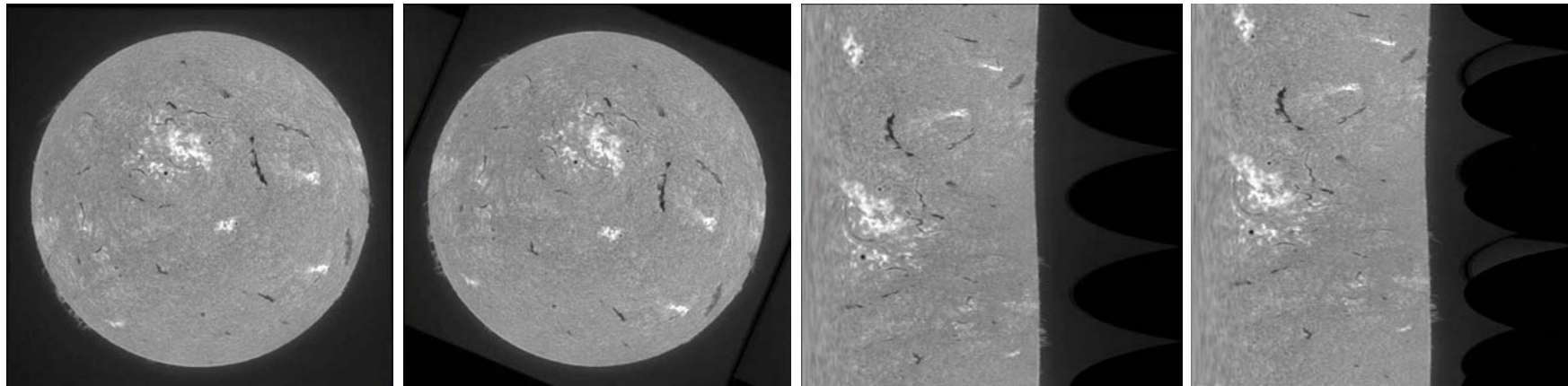
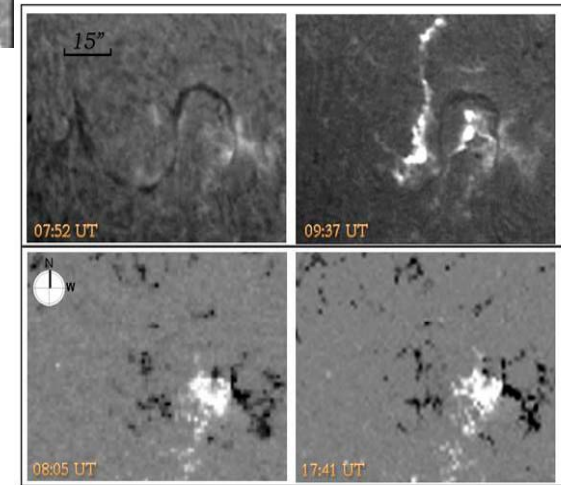
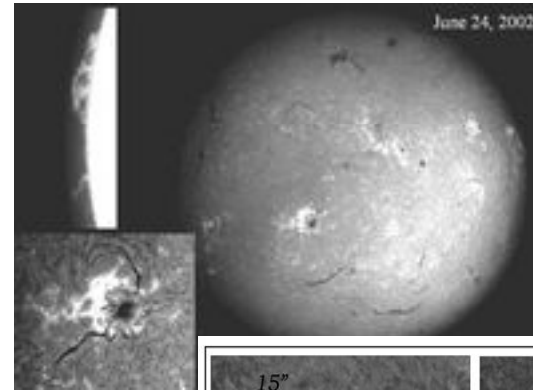
The features given hardware-programme complex do its irreplaceable at decision of the problems solar physicists. It also can be used for processing existing database of the observations Baykal Astrophysical Observatory that will enable to get generalising given on perennial observations Sun.

Numerical processing of images of solar chromosphere

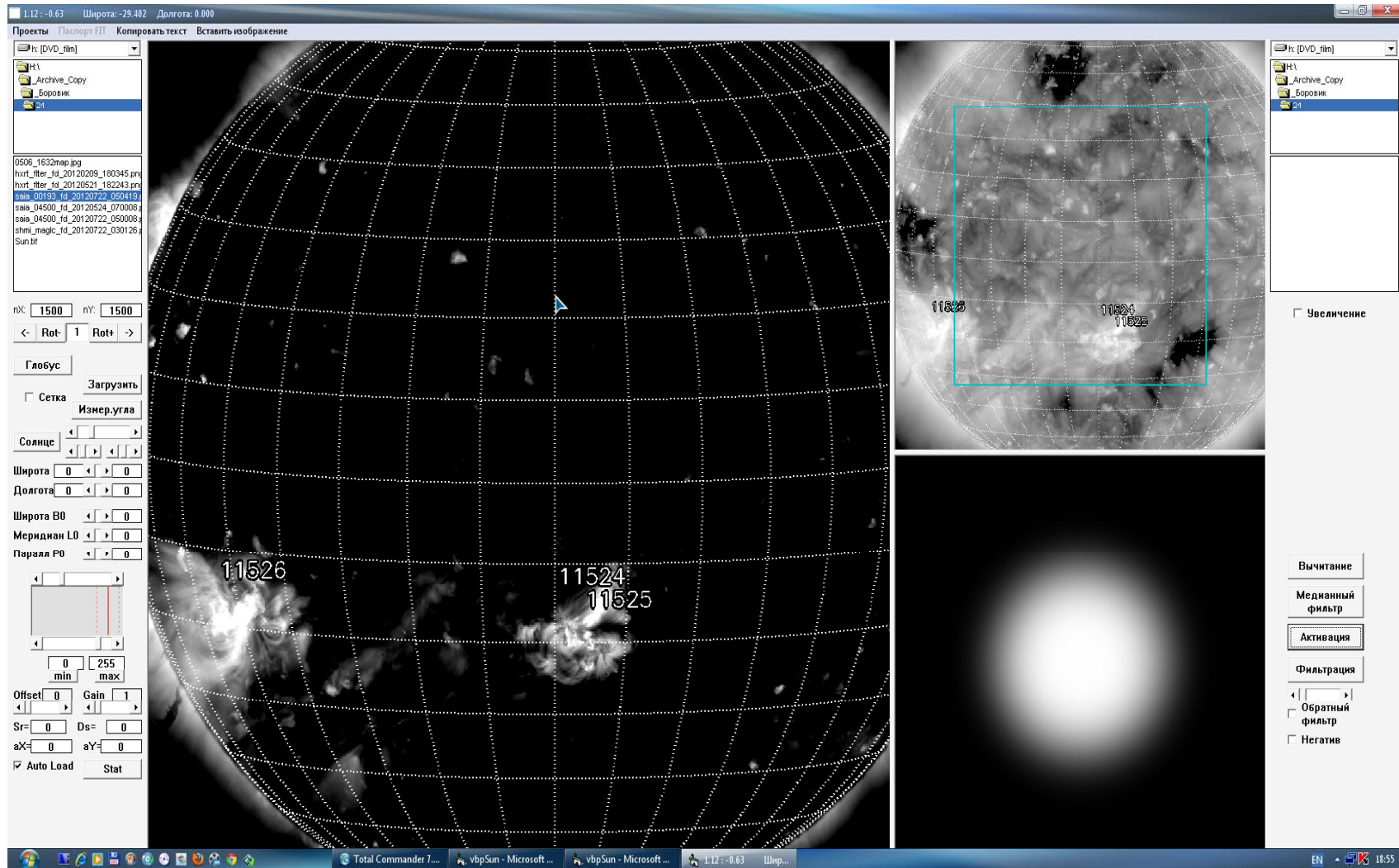
List of problems

- analysis of images and choose the best image in different formats and transformations,
- correction of instrumentation and atmospheric distortions, calibration, and high precision co-ordination of images,
- spherical transformation details on Sun surface with scale changing, measure of angular of rotation, coefficient of scaling,
- cortensial transformation of images – rotation, scaling, displacement,
- space-temporal correlation and spectral analysis of images.

$$R(\theta) = \begin{pmatrix} \cos \theta & -\sin \theta \\ \sin \theta & \cos \theta \end{pmatrix} = \begin{pmatrix} 1 & -\tan \theta / 2 \\ 0 & 1 \end{pmatrix} \times \begin{pmatrix} 1 & 0 \\ \sin \theta & 1 \end{pmatrix} \times \begin{pmatrix} 1 & -\tan \theta / 2 \\ 0 & 1 \end{pmatrix}$$



Picture frame of HPC



Dynamic characteristics of adaptive systems

- A common adaptive system with a finite frequency band (or a finite response time) is described as a dynamic constant time-delay system, where time delay is to be much shorter than the time of coherence radius transfer through an telescope aperture by a mean wind speed.
- The questions of the image formation are considered with use the reference source.
- The analytical calculation of the Strehl parameter is made on base of the generalized principle of Huygens–Kirchhoff.
- An adaptive system is considered, where the correcting phase is calculated with the use of both its derivatives and the signal, as well as adaptive systems using different time predicting algorithms of correcting signal for future time points.
- The use of a predicted phase front of the correcting wave allows much longer time delays.
- The stronger phase distortions in the optical wave the higher time gain in comparison with common (with constant time-delay) adaptive system.

Development of algorithms of forecasting correction

Phase fluctuation evolution on small time interval presented as a truncated Taylor's expansion:

$$\widehat{S}(\vec{\rho}, t + \tau) = S(\vec{\rho}, t) + \dot{S}(\vec{\rho}, t)\tau + \ddot{S}(\vec{\rho}, t)\tau^2 / 2!$$

1. Traditional scheme of correction

$$\widehat{S}(\vec{\rho}, t + \tau) = S(\vec{\rho}, t) \longrightarrow \tau_1 < 0.53 \left(\frac{r_0}{v}\right) (2R / r_0)^{1/6}$$

2. "Fast" correction

$$\widehat{S}(\vec{\rho}, t + \tau) = S(\vec{\rho}, t) + \nabla_{\vec{\rho}} S(\vec{\rho} + \vec{v}\tau, t) \Big|_{\vec{\rho}=0} \cdot \vec{v}\tau$$

$\tau_2 < 0.59 \left(\frac{r_0}{v}\right) (2R / r_0)^{7/12}$

$$\tau_2 / \tau_1 \approx (2R / r_0)^{5/12}$$

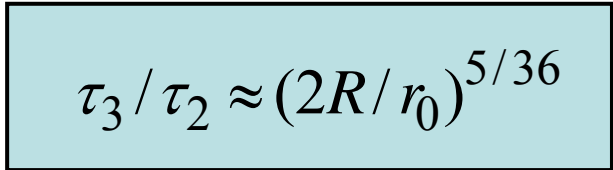
Algorithms of forecasting correction

Phase fluctuation evolution on small time interval presented as a truncated Taylor's expansion:

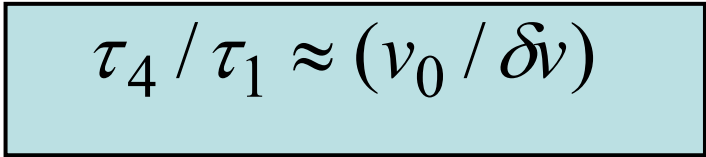
$$\hat{S}(\vec{\rho}, t + \tau) = S(\vec{\rho}, t) + \dot{S}(\vec{\rho}, t)\tau + \ddot{S}(\vec{\rho}, t)\tau^2 / 2!$$

3. Correction with acceleration

$$\hat{S}(\vec{\rho}, t + \tau) = S(\vec{\rho}, t) + \nabla_{\vec{\rho}} S(\vec{\rho}, t) \Big|_{\vec{\rho}=0} \cdot \vec{v} \tau + \nabla_{\vec{\rho}}^2 S(\vec{\rho}, t) \Big|_{\vec{\rho}=0} \cdot v^2 \tau^2 / 2!$$

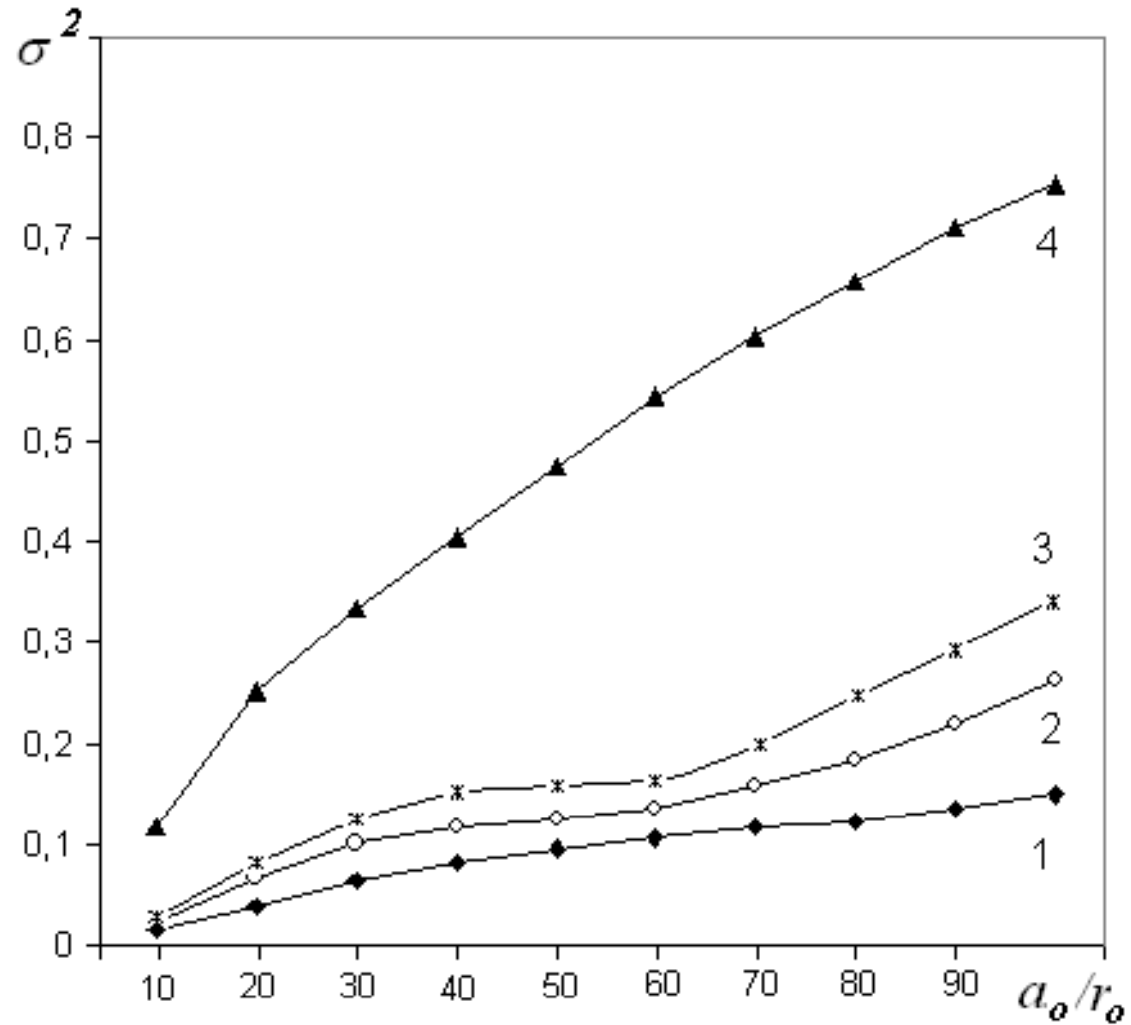

$$\tau_3 / \tau_2 \approx (2R / r_0)^{5/36}$$

4. Correction on the base of “frozen fluctuations” model

$$\hat{S}(\vec{r}, t + \tau) = S(\vec{r} + \vec{v}_0 \tau, t)$$

$$\tau_4 / \tau_1 \approx (v_0 / \delta v)$$

$$(\langle [\vec{v} - \vec{v}_0]^2 \rangle)^{1/2} = \delta v$$

Variances of residual error of wavefront estimation as a function of intensity of turbulent distortions for different temporal delay (curves 1-3), 4 – without forecasting.



Spectral characteristics of adaptive systems

